

SANDIA REPORT

SAND2009-2817
Unlimited Release
Printed R } ^ 2009

Photoneutron Effects on Pulse Reactor Kinetics for the Annular Core Research Reactor (ACRR)

Edward J. Parma

Prepared by
Sandia National Laboratories
Albuquerque, New Mexico 87185 and Livermore, California 94550

Sandia is a multiprogram laboratory operated by Sandia Corporation, a Lockheed Martin Company, for the United States Department of Energy's National Nuclear Security Administration under Contract DE-AC04-94AL85000.

Approved for public release; further dissemination unlimited.

Issued by Sandia National Laboratories, operated for the United States Department of Energy by Sandia Corporation.

NOTICE: This report was prepared as an account of work sponsored by an agency of the United States Government. Neither the United States Government, nor any agency thereof, nor any of their employees, nor any of their contractors, subcontractors, or their employees, make any warranty, express or implied, or assume any legal liability or responsibility for the accuracy, completeness, or usefulness of any information, apparatus, product, or process disclosed, or represent that its use would not infringe privately owned rights. Reference herein to any specific commercial product, process, or service by trade name, trademark, manufacturer, or otherwise, does not necessarily constitute or imply its endorsement, recommendation, or favoring by the United States Government, any agency thereof, or any of their contractors or subcontractors. The views and opinions expressed herein do not necessarily state or reflect those of the United States Government, any agency thereof, or any of their contractors.

Printed in the United States of America. This report has been reproduced directly from the best available copy.

Available to DOE and DOE contractors from
U.S. Department of Energy
Office of Scientific and Technical Information
P.O. Box 62
Oak Ridge, TN 37831

Telephone: (865) 576-8401
Facsimile: (865) 576-5728
E-Mail: reports@adonis.osti.gov
Online ordering: <http://www.osti.gov/bridge>

Available to the public from
U.S. Department of Commerce
National Technical Information Service
5285 Port Royal Rd.
Springfield, VA 22161

Telephone: (800) 553-6847
Facsimile: (703) 605-6900
E-Mail: orders@ntis.fedworld.gov
Online order: <http://www.ntis.gov/help/ordermethods.asp?loc=7-4-0#online>



SAND2009-2817
Unlimited Release
Printed Lwpg 2009

Photoneutron Effects on Pulse Reactor Kinetics for the Annular Core Research Reactor (ACRR)

Edward J. Parma
Sandia National Laboratories
P.O. Box 5800
Albuquerque, NM 87185-1136

Abstract

The Annular Core Research Reactor (ACRR) is a swimming-pool type pulsed reactor that maintains an epithermal neutron flux and a nine-inch diameter central dry cavity. One of its uses is neutron and gamma-ray irradiation damage studies on electronic components under transient reactor power conditions. In analyzing the experimental results, careful attention must be paid to the kinetics associated with the reactor to ensure that the transient behavior of the electronic device is understood. Since the ACRR fuel maintains a substantial amount of beryllium, copious quantities of photoneutrons are produced that can significantly alter the expected behavior of the reactor power, especially following a reactor pulse. In order to understand these photoneutron effects on the reactor kinetics, the KIFLE transient reactor-analysis code was modified to include the photoneutron groups associated with the beryllium. The time-dependent behavior of the reactor power was analyzed for small and large pulses, assuming several initial conditions including following several pulses during the day, and following a long steady-state power run. The results indicate that, for these types of initial conditions, the photoneutron contribution to the reactor pulse energy can have a few to tens of percent effect.

CONTENTS

1	Introduction.....	5
2	Analysis Approach.....	7
3	Results.....	9
	3.1 <i>Single Pulse</i>	10
	3.2 <i>Multiple Pulses</i>	15
	3.3 <i>Pulse Following a Steady-State Power Run</i>	19
4	Conclusions.....	22
5	References.....	23

TABLES

Table 1. Delayed Photoneutron 9-Group Constants from Keepin.....	8
Table 2. Delayed 8-Group Constants from Campbell and Spriggs	8

FIGURES

Figure 1. The Annular Core Research Reactor.....	5
Figure 2. ACRR Power as a Function of Time for a \$3.16 Pulse With and Without Photoneutrons – Log-Log Scale.	11
Figure 3. ACRR Power as a Function of Time for a \$3.16 Pulse With and Without Photoneutrons – Log-Linear Scale.	12
Figure 4. ACRR Power as a Function of Time for a \$3.16 Pulse With and Without Photoneutrons – Linear-Linear Scale.	12
Figure 5. ACRR Power Integrated Over Time as a Function of Time for a \$3.16 Pulse after 300 Seconds – Photoneutron Result Minus Nominal Result.	13
Figure 6. ACRR Power as a Function of Time for a \$1.35 Pulse With and Without Photoneutrons – Log-Log Scale.	14
Figure 7. ACRR Power as a Function of Time for a \$1.35 Pulse With and Without Photoneutrons Following a Series of Pulses – Log-Log Scale.	16
Figure 8. ACRR Power as a Function of Time for a \$3.16 Pulse With and Without Photoneutrons Following a Series of Pulses – Log-Log Scale.	17
Figure 9. ACRR Power Integrated Over Time as a Function of Time for a \$1.35 Pulse after 300 Seconds – Photoneutron Result Minus Nominal Result.	17
Figure 10. ACRR Power Integrated Over Time as a Function of Time for a \$3.16 Pulse after 300 Seconds – Photoneutron Result Minus Nominal Result.	18
Figure 11. ACRR Power as a Function of Time for a \$1.35 Pulse With and Without Photoneutrons Following 2 MW Steady-State Power Run – Log-Log Scale.	20
Figure 12. ACRR Power as a Function of Time for a \$3.16 Pulse With and Without Photoneutrons Following 2 MW Steady-State Power Run – Log-Log Scale.	20
Figure 13. ACRR Power Integrated Over Time as a Function of Time for a \$1.35 Pulse after 300 Seconds – Photoneutron Result Minus Nominal Result.	21
Figure 14. ACRR Power Integrated Over Time as a Function of Time for a \$3.16 Pulse after 300 Seconds – Photoneutron Result Minus Nominal Result.	21

1 INTRODUCTION

The Annular Core Research Reactor (ACRR) is a swimming-pool type research reactor that is capable of operating in a pulse, transient, or steady-state mode. Shown in Figure 1, the ACRR maintains a dry central cavity, nine inches in diameter, that passes from the top of the pool through the center of the core. The dry cavity allows for relatively large experiment packages to be placed at the center of the core for irradiation at the peak neutron flux. The neutron flux in the reactor core and cavity is epithermal. The ACRR can be operated at 4 MW continuous power level in a steady-state mode, or 300 MJ energy deposition in a pulse or transient mode. The pulse operating conditions for ACRR are several times that which can be achieved in a typical TRIGA-type university reactor. The ACRR maintains a special fuel type made up of uranium oxide (UO_2) and beryllium oxide (BeO). The fuel was designed with the BeO to allow for a high heat capacity and enhanced pulsing capabilities in the reactor. The ACRR is the only research reactor in the world that uses this fuel type. The Be in the fuel produces copious quantities of photoneutrons. These photoneutrons create a significant neutron population that always exists at some level in the reactor core and allows for the reactor to be operated without an external neutron source.

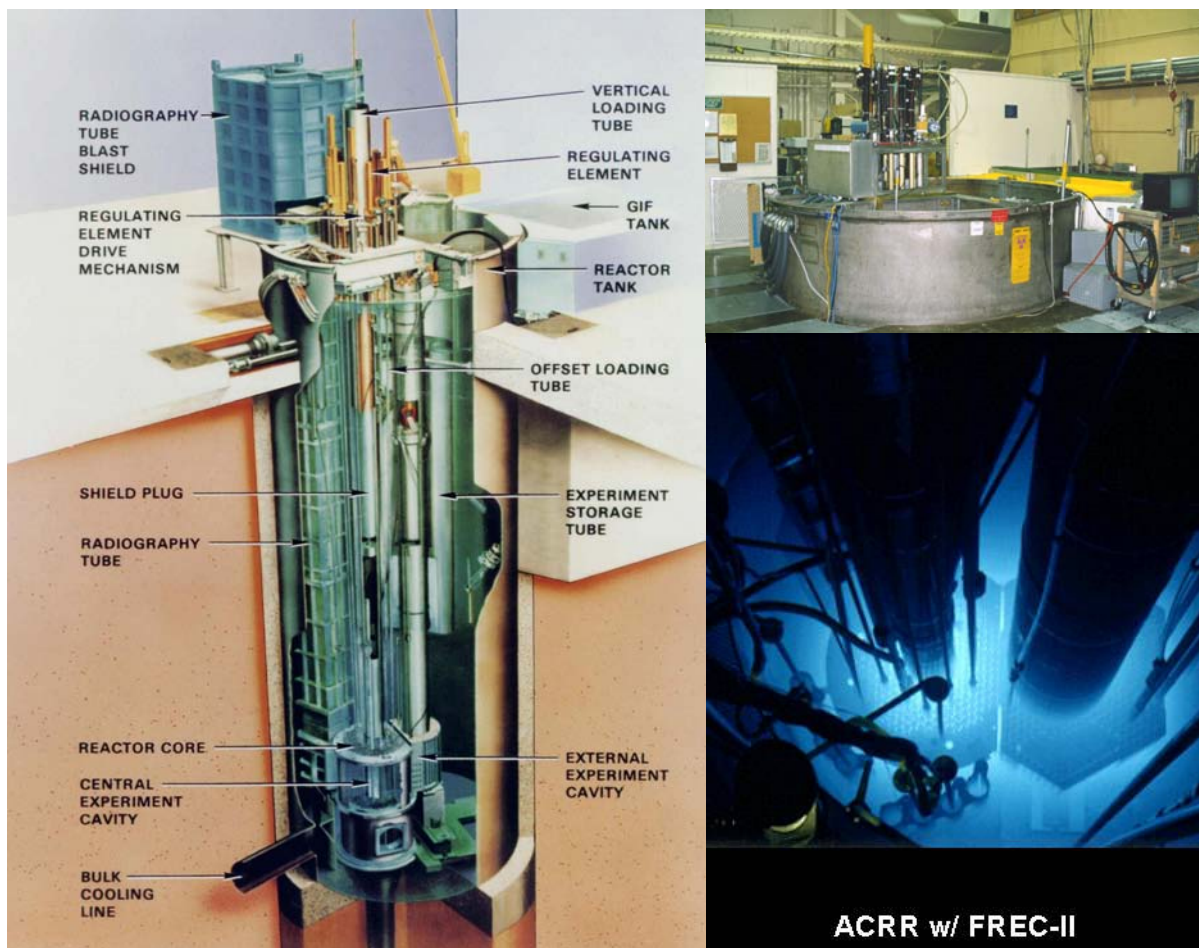


Figure 1. The Annular Core Research Reactor.

Be photoneutron production is discussed in detail in Keepin (1964). A Be photoneutron is generated when a gamma ray, with energy above the threshold energy (1.7 MeV), interacts with a Be-9 nucleus causing a (γ, n) reaction. The gamma rays can be produced from fission, decay of fission products, or (n, γ) reactions. The photoneutrons created as a result of fission product decay gammas can be treated as additional delayed neutron groups in the point-reactor kinetics equations. The amount of photoneutrons generated in this process is relatively small compared to the normal delayed neutrons, representing only an additional 2% to the value for the total delayed neutron fraction, β . For thermal U-235 fission, β is 0.007. The contribution from the additional photoneutrons is ~ 0.00015 . The reason that these photoneutrons can be treated as additional delayed neutron groups is because they are generated by fission product decay, similar to delayed neutron precursors, which are decaying fission products that give off neutrons.

From an operational perspective, the photoneutrons can be ignored for reactivity measurements because they represent such a small fraction of β . That is, these additional groups are not considered in the inhour equations in transforming the stable reactor period to reactivity. Neglecting the photoneutrons will present a small bias error in reactivity measurements.

The presence of the photoneutrons does affect the minimum critical power level that can be achieved for the reactor. The minimum power level is determined by the background photoneutron source that exists at the time of the operation. Typically, the minimum delayed critical power level is ~ 1200 watts (W). Lower levels can be achieved after prolonged periods of reactor shutdown.

A reactor pulse will be affected in two ways by the presence of the photoneutrons. First, the delayed critical condition can be masked by the photoneutron population prior to the pulse. Second, the photoneutron population prior to and during the pulse will cause the tail portion of the pulse to be at a higher power level than if the photoneutrons were not present. This can cause dosimetry response in the central cavity to be greater than expected if nominal neutron kinetics are used to determine the reactor power level in the tail portion of a pulse. These two effects will be the primary focus of this work.

One use for ACRR is neutron and gamma-ray irradiation damage studies on electronic components under transient reactor power conditions. In analyzing the experimental results, careful attention must be paid to the kinetics associated with the reactor to ensure that the transient behavior of the electronic device is understood, since the photoneutrons produced can significantly alter the expected behavior of the reactor power, especially following a reactor pulse. In order to understand these photoneutron effects on the reactor kinetics, the KIFLHE transient reactor analysis code was modified to include the photoneutron groups associated with the Be. The time-dependent behavior of the reactor power was analyzed for small and large pulses assuming several initial conditions including, following several pulses during the day, and following a long steady-state power run.

2 ANALYSIS APPROACH

The computer code, KIFLHE, is a transient reactor-analysis code used to analyze ACRR power transients under pulsed and steady-state conditions. KIFLHE has been used extensively to study reactivity transients and accident conditions for the ACRR (Parma, 2000; Naegeli, 1999; Naegeli, 2000). The code solves the point-reactor kinetics equations, two-dimensional heat transfer (R-Z) in a fuel element, and one-dimensional fluid flow (Z) in a flow channel. The kinetics equations are solved using the Laplace transform method. The roots of the inhour equation are numerically derived and the power level calculated. The advantage of using the Laplace transform method over the Runge-Kutta method to solve the equations is that the time steps can be of any size as long as the reactivity is not changing over that time period. The Laplace transform methodology will provide no advantage for pulse conditions, where short time steps are required for the rapid reactivity changes due to the pulse rod insertion and reactor feedback. However, over long time periods of constant reactivity, large time steps can be taken without penalty in the accuracy of the calculation.

The point-kinetics portion of the KIFLHE code originally contained the 6-delayed neutron groups for thermal U-235 fission given in Lewins (1978). In order to analyze the photoneutron effects, the 9-group photoneutron precursor constants found in Keepin (1964) were used along with the 8-group precursor constants of Campbell and Spriggs (1999). The 8-group (U-235 thermal) constants from Campbell and Spriggs were included in the code since they represent recent work in this area. There should be no significant difference in the results from using the historical 6-delayed neutron groups compared to the 8-group data. The 8-group constants have the advantage that the group half-lives are constant for fast versus thermal and for the different fissile isotopes. Only the delayed precursor fractions change for the 8-group data, which allows for convenient computation of the delayed fraction for mixtures of fissile isotopes including fast and thermal fission.

The 9-group photoneutron precursor constants from Keepin are shown in Table 1. The U-235 thermal 8-group precursor constants from Campbell and Spriggs are shown in Table 2. Note that the total group fraction for the photoneutrons (15.175×10^{-5}) is about 2% of the delayed fraction for U-235 thermal fission (0.007). The longest half-life precursor for the delayed neutrons (Table 2) is 55.6 seconds. The time constant for this precursor ($\tau = T_{1/2}/\ln 2$) is 80.2 seconds, which is the shutdown time constant for a nuclear reactor. That is, after a nuclear reactor is operated and then shut down with a large negative reactivity insertion, the power level decreases with this time constant (80.2 sec), independent of the amount of negative reactivity added. However, for the ACRR, this will not be the case due to the photoneutron population.

The longest lived photoneutron precursor in Table 1 is shown to have a half-life of 12.8 days. In previous unreferenced work, the author has found that an additional longer-lived precursor group exists, with a half-life of 369 days, which is not presented in the Keepin data. Note that in Table 1, the longest-lived photoneutron precursor that has a significant group fraction is precursor number four with a half-life of 3.11 hours. This precursor dominates the daily variation in the ACRR neutron source along with the longer-lived precursors (numbers one through three), providing the more constant background neutron source level. The shortest-lived photoneutron precursor is 30.6 seconds, which is close to the longest-lived delayed neutron precursor.

Table 1. Delayed Photoneutron 9-Group Constants from Keepin.

Group Number	Half-Life	λ_i (s ⁻¹)	Group Fraction b_i (10 ⁻⁵)
1	12.8 d	6.24E-7	0.057
2	77.7 h	2.48E-6	0.038
3	12.1 h	1.59E-5	0.260
4	3.11 h	6.20E-5	3.20
5	43.2 m	2.67E-4	0.36
6	15.5 m	7.42E-4	3.68
7	3.2 m	3.60E-3	1.85
8	1.3 m	8.85E-3	3.66
9	30.6 s	2.26E-2	2.07
total	--	--	15.175

Table 2. Delayed 8-Group Constants from Campbell and Spriggs for U-235 Thermal Fission.

Group Number	Half-Life	λ_i (s ⁻¹)	Group Fraction b_i (10 ⁻³)
1	55.6 s	1.25E-2	0.231
2	24.5 s	2.83E-2	1.078
3	16.3 s	4.25E-2	0.637
4	5.21 s	1.33E-1	1.379
5	2.37 s	2.92E-1	2.317
6	1.04 s	6.66E-1	0.630
7	0.424 s	1.63E-0	0.567
8	0.195 s	3.55E-0	0.161
total	--	--	7.00

The modifications required to the KIFLHE code, in order to include these additional delayed group constants, turned out to be only a few minor changes. The code now has the ability to run the 6-group Lewins (U-235 thermal) values, the 8-group Campbell and Spriggs (U-235 thermal) values, or a combination of the 8-group Campbell and Spriggs values with the 9-group Keepin Be photoneutron values. It is unclear as to how accurate the Keepin photoneutron group fraction values are in relation to the ACRR. The values are shown in Keepin to represent experimental results accurately. However, the gamma-to-neutron conversion effectiveness and the neutron effectiveness factors for ACRR are unknown. Further work using MCNP could allow a more accurate representation of the group fractions to be determined for ACRR. It is believed that the values for the group fractions presented in Keepin represent the largest values possible. Hence it is expected that the calculative results represent an overestimate of their effect on the kinetic behavior of the reactor. Also, the delayed neutron contribution from U-235 and U-238 fast fission was not included in the KIFLHE calculations. Although expected to be small, these contributions could change the group fractions slightly. This contribution would not be expected to have any major significance on the results, although future work could include MCNP calculations to determine the fast fission contribution to the reactor power and associated delayed neutron contribution. β effective used in the KIFLE calculations was 0.0073, which has historically been used for ACRR.

3 RESULTS

KIFLHE calculations were run both with and without the photoneutron delayed group contribution. Two pulse conditions were studied: a large pulse where \$3.16 of reactivity was added resulting in ~280MJ of reactor energy deposition; and a small pulse where \$1.35 of reactivity was added resulting in ~38 MJ of reactor energy deposition. These conditions represent typical values for a large and small pulse, respectively. Three initial conditions were considered prior to the pulse: 1) no initial contribution from photoneutrons; 2) photoneutron population from several pulses during the day; and 3) photoneutron population from a long steady-state power operation.

3.1 *Single Pulse*

Single pulse analyses were performed to determine the effects of the photoneutrons on the pulse transient, without a prior photoneutron population. This case represents the “clean core” condition found during the first pulse of the day or following a weekend shutdown. KIFLHE calculations, both with and without the photoneutron delayed groups, were run using the following conditions. These conditions were derived from discussions with ACRR operations staff and represent typical pulse conditions.

- Initial reactivity condition = \$0.00 (delayed critical condition)
- Initial power level = 1200 W
- Pulse reactivity insertion = \$3.16 (representing a large pulse - 280 MJ)
\$1.35 (representing a small pulse - 38 MJ)
- Reactivity insertion duration = 0.11 sec
- Shutdown reactivity = -\$11.50
- Negative reactivity insertion duration = 0.5 sec
- Start time of pulse = 5.1 sec (arbitrarily chosen in the code)
- Start time of reactor shutdown = 5.34 s (0.24 sec following start of reactivity insertion)

The initial steady-state inventory for the delayed neutron and delayed photoneutron precursors was set to correspond to a steady-state power level of 1200 W that represents the critical condition established prior to the pulse. This condition places all of the delayed precursors, both nominal and photoneutron, in equilibrium at 1200 W prior to the pulse. Although reasonable for the nominal delayed neutrons, this condition may not be realistic for the photoneutron precursors, since photoneutron groups one to five have relatively long half-lives and would take several hours at this power level to reach equilibrium. In order to assess this effect on the reactor power, a separate case was studied whereby only the short-lived photoneutron precursors were placed in equilibrium at 1200 W.

Results for a Large Pulse

Figures 2 to 4 show the results of the calculated reactor power as a function of time with and without the photoneutrons included in the large \$3.16 pulse. The results are virtually identical for the pulse portion of the curve, with the deviation in the tail due to the longer-lived photoneutron effects.

- Peak power = 23,800 MW
- Time at peak = 5.196 sec (0.096 sec following start of reactivity insertion)
- FWHM = 9 ms
- Total Energy = ~280 MJ (pulse and tail)

For the calculation without photoneutrons, the reactor power drops below 100 W at 404 s (6.7 min), and below 10 W at 590 s (9.8 min). With photoneutrons, the reactor power drops below 100 W at 890 s (14.8 min), and below 10 W at 6235 s (103.9 min). It can be seen in Figures 3 and 4 that the photoneutrons begin to become important and deviate from the nominal delayed neutron case at ~300 s (5 min.), when the reactor power is ~1000 W. After ~10,000 s (2.8 hours), the power level is dominated, for the “with photoneutron” case, by the fourth photoneutron precursor that has a half-life of 3.11 hours.

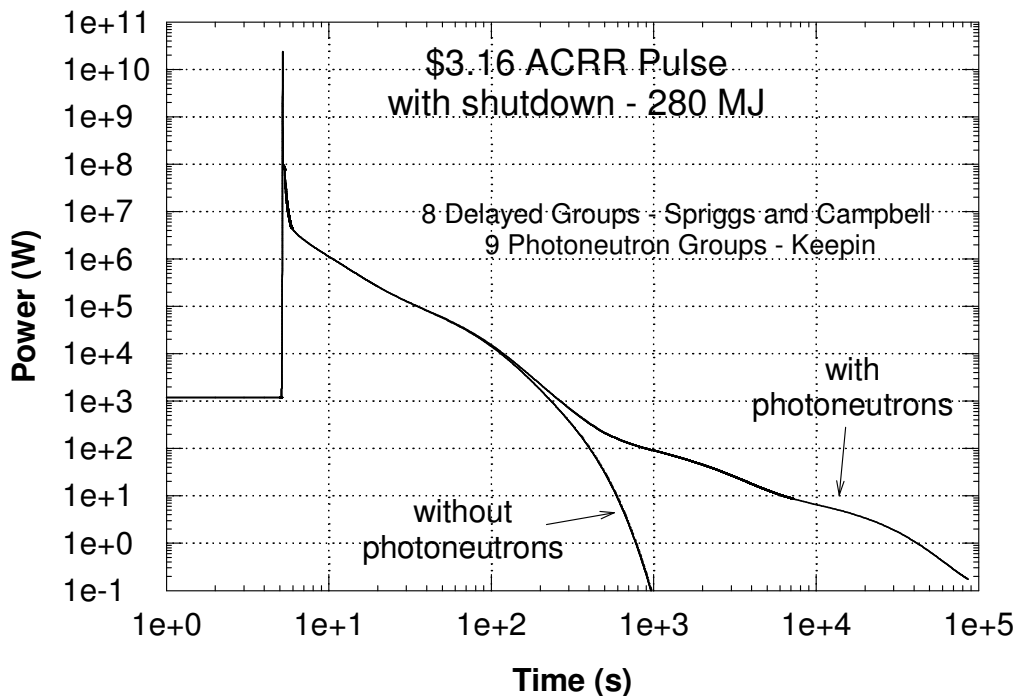


Figure 2. ACRR Power as a Function of Time for a \$3.16 Pulse With and Without Photoneutrons – Log-Log Scale.

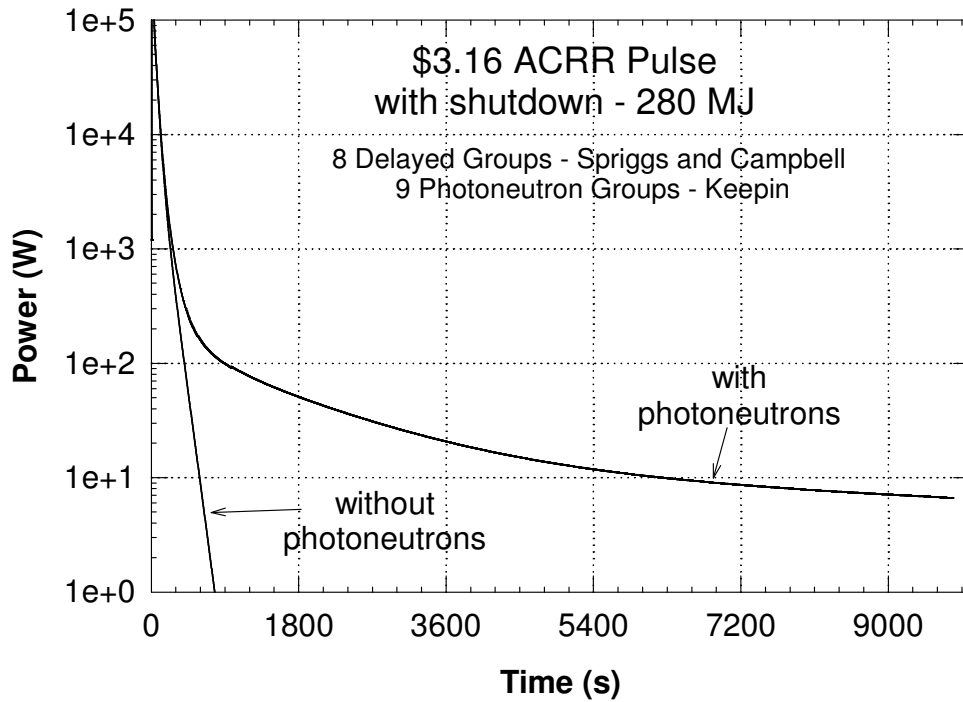


Figure 3. ACRR Power as a Function of Time for a \$3.16 Pulse With and Without Photoneutrons – Log-Linear Scale.

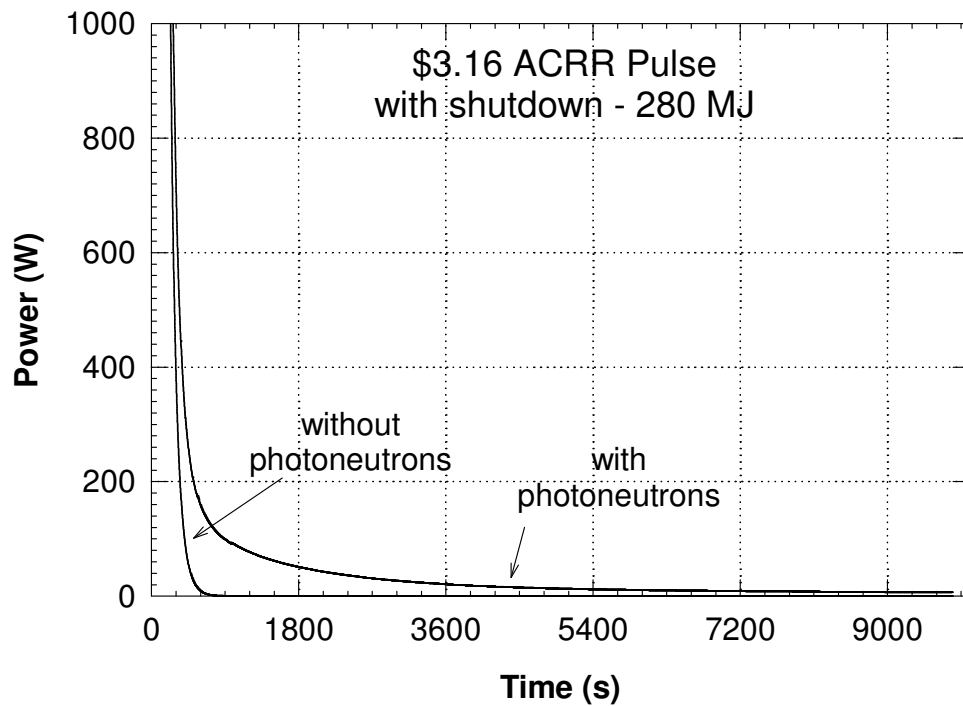


Figure 4. ACRR Power as a Function of Time for a \$3.16 Pulse With and Without Photoneutrons – Linear-Linear Scale.

Figure 5 shows the time-integrated difference in the reactor power (energy as a function of time resulting from the photoneutron case minus nominal result) after 300 s. At 10,000 s (2.8 hours) the amount of energy deposited in the core due to the photoneutron effects is ~0.3 MJ. Comparing this result to the 280 MJ total pulse energy represents about 0.1% of the total energy deposited in the pulse. Since the photoneutron precursor concentration is dependent on the number of fissions that occurred in the pulse, a smaller pulse would yield a proportionately smaller precursor concentration and proportionally lower power level and energy in the tail. Hence for all pulses, the additional energy deposited in the tail from the photoneutrons should be ~0.1%. The timing for the photoneutron importance should be the same as described above.

Another calculation was performed to determine the effects of not having any of the long-lived photoneutron precursors (group numbers 1-5) in an initial state of equilibrium in the calculation. Since the photoneutron precursors in these groups have relatively long half-lives, they would not be expected to be in equilibrium for the first pulse of the day. The precursor values were initially zeroed for groups 1-5 for this calculation. The results showed only a 10% effect on the reactor power at late times. This result confirms what one would intuitively expect, that, like for delayed precursors, the photoneutron precursor concentration is dominated by the fission products produced in the pulse and not the low steady-state power level prior to the pulse.

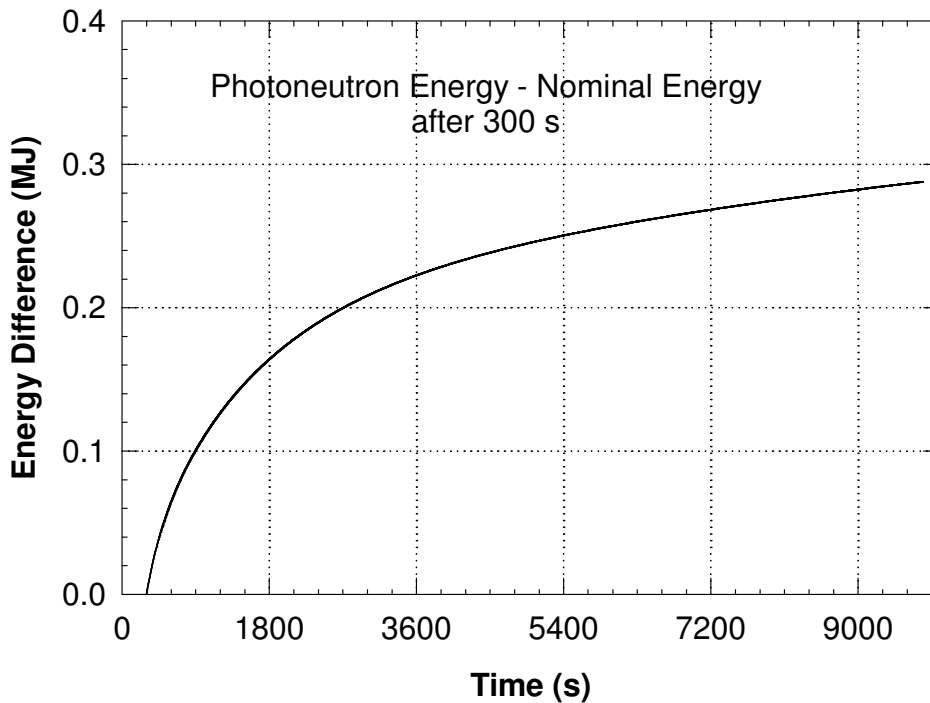


Figure 5. ACRR Power Integrated Over Time as a Function of Time for a \$3.16 Pulse after 300 Seconds – Photoneutron Result Minus Nominal Result.

Results for a Small Pulse

Figure 6 shows the results of the calculated reactor power as a function of time with and without the photoneutrons included in the small \$1.35 pulse. The results are again virtually identical for the pulse portion of the curve, with the deviation in the tail due to the longer-lived photoneutron effects.

- Peak power = 859 MW
- Time at peak = 5.259 sec (0.159 sec following start of reactivity insertion)
- FWHM = 35 ms
- Total Energy = ~38 MJ (pulse and tail)

For the calculation without photoneutrons, the reactor power drops below 100 W at 255 s (4.3 min), and below 10 W at 425 s (7.1 min). With photoneutrons, the reactor power drops below 100 W at 290 s (4.8 min), and below 10 W at 1136 s (18.9 min). The results are similar to the large pulse results. The photoneutrons again begin to become important and deviate from the nominal delayed neutron case at ~300 s (5 min.), when the reactor power is ~100 W. After ~10,000 s (2.8 hours), the power level is dominated, for the “with photoneutron” case, by the fourth photoneutron precursor that has a half-life of 3.11 hours. The photoneutron results in the tail for the small pulse case are approximately an order of magnitude less than for the large pulse, as would be expected.

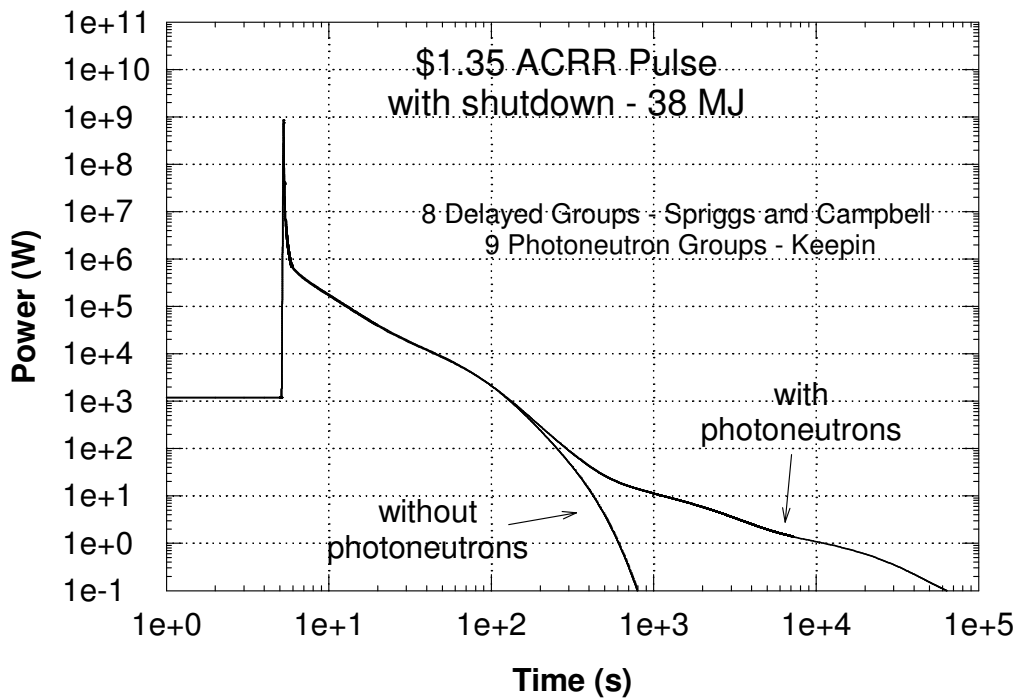


Figure 6. ACRR Power as a Function of Time for a \$1.35 Pulse With and Without Photoneutrons – Log-Log Scale.

3.2 *Multiple Pulses*

The background photoneutron inventory will change throughout the course of a day's operational history of the ACRR due to the long-lived photoneutron precursors in groups one through five (Table 1). Both power runs and multiple pulses during the day will change the inventory. The background photoneutron inventory affects both the pulse setup conditions and the pulse tail power trace. After multiple pulses during the day or a long duration power run, the pulse setup becomes problematic because delayed critical is established at a low steady-state power level prior to the pulse. The larger background photoneutron source "masks" the "true" delayed critical condition of the reactor by several cents of reactivity. The effect of this masking condition is that the control rods are set, not at "true" delayed critical, but at a delayed subcritical state. For reactors where a moveable source can be inserted or removed from the core, this condition is known as "source critical." If the reactor is placed in what is thought to be a delayed critical condition and the source is removed from the core, the reactor will actually be in a subcritical state by several cents of reactivity. This can be shown to be true analytically by solving the point-reactor kinetics equations with a source. At the critical condition with a source in place, the reactor maintains a slight positive period equivalent to a few cents of reactivity, dependent on the source strength and position in the core.

The photoneutron source effect on the ACRR is that the reactivity inserted from the pulse rods will be "short" of the desired reactivity insertion by a few cents. The effect will vary from pulse to pulse, building up after many pulses in a day or after a long power run. This "reactivity cheating" effect for pulses at the ACRR has been observed by Depriest (2008) and for transient rod withdrawal operations by the author. The effect on the pulse tail is that the tail power level will continue to increase proportionately with the amount of energy deposited in the core during the day. However, after several hours with the reactor in a shutdown condition, the background photoneutron effects diminish. In Table 1, the fourth photoneutron precursor can be seen to have a relatively large group fraction, compared to groups one, two, and three. The half-life of the fourth group photoneutron precursor is 3.11 hours. At about five half-lives following the last reactor operation of the day (~15 hours), this precursor group will have decayed to virtually zero, and the photoneutron background will be significantly diminished. This is typically observed at the ACRR. The first pulse of the day has a significantly smaller source strength during the delayed critical setup. Nothing can be done to change the tail behavior of the pulse, except to minimize it by utilizing the first pulse of the day. The "reactivity cheating" effects can be controlled by setting the control rod positions at the same values as delayed critical position for the first pulse of the day. However, when this is done, the reactor will be on a slightly positive period, due to the photoneutron source, prior to the pulse reactivity insertion. Another method would be to set the control rods such that the reactor is slightly subcritical for the first pulse of the day (5 to 10 cents negative) and maintaining this setup position for every pulse during the day. The caveat is that this method will only work if the experiment package reactivity does not change from one pulse to the next.

KIFLHE calculations were performed to determine the pulse tail effects for a pulse following a series of large pulses. Figures 7 and 8 show the results for a \$1.35 pulse (38 MJ) and a \$3.16 pulse (280 MJ) following a series of three \$3.16 pulses, two hours apart. The calculations were performed in the same method as for a single pulse. In order to have the correct photoneutron precursor inventory at the start of the pulse, the precursor inventory values, after a 2-hour decay

from the previous pulse, were used as the initial precursor inventory for the calculation. The tail is at a higher power level for the multiple pulse cases as compared to the single pulse. For the \$1.35 pulse case, the power level is about an order of magnitude greater between 2 and 15 hours following the pulse as compared to Figure 6. For the \$3.16 pulse, the power level is only about a factor of two larger than the values in Figure 2.

Figure 9 shows the integrated power level difference for the \$1.35 pulse case, both with and without previous pulses. At 24 hours, the energy deposition is 0.24 MJ and 0.06 MJ, for the multiple pulse and single pulse, respectively. The value is a factor of four larger for the multiple pulse series, but still only represents 0.6% of the energy deposited in the pulse.

Figure 10 shows the integrated power level difference for the \$3.16 pulse case, both with and without previous pulses. At 24 hours, the energy deposition is 0.61 MJ and 0.40 MJ, for the multiple pulse and single pulse, respectively. The value is a factor of 1.5 larger for the multiple pulse series, but still only represents 0.2% of the energy deposited in the pulse.

The results clearly show that multiple pulses prior to a pulse do have an effect on the tail portion of the pulse. However, the magnitude of this value with respect to the energy deposited in the pulse is found to be less than 1%.

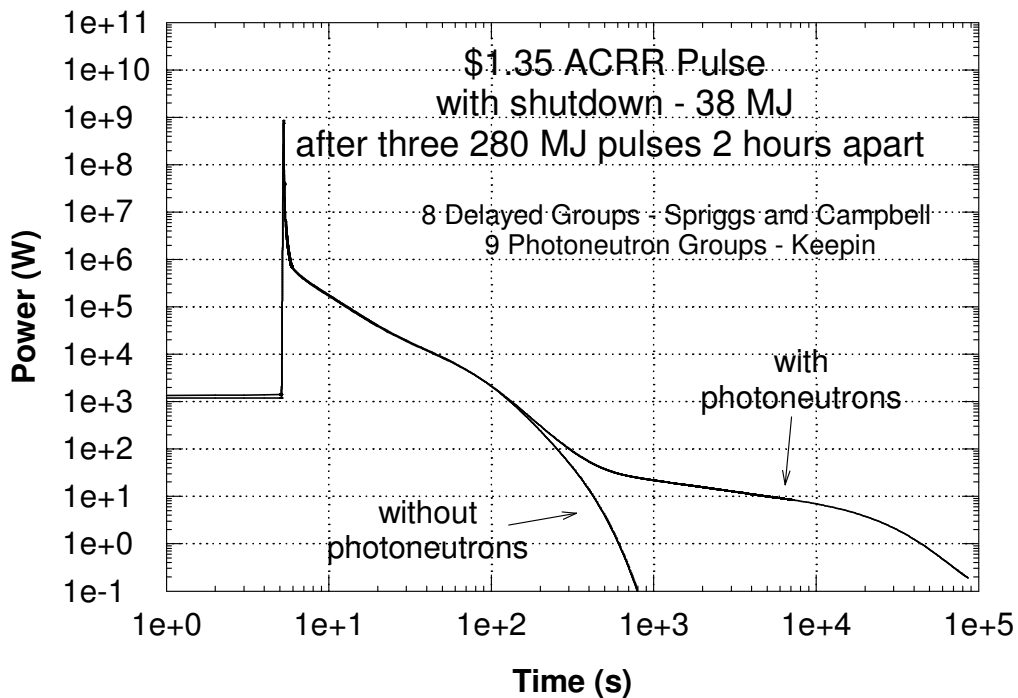


Figure 7. ACRR Power as a Function of Time for a \$1.35 Pulse With and Without Photoneutrons Following a Series of Pulses – Log-Log Scale.

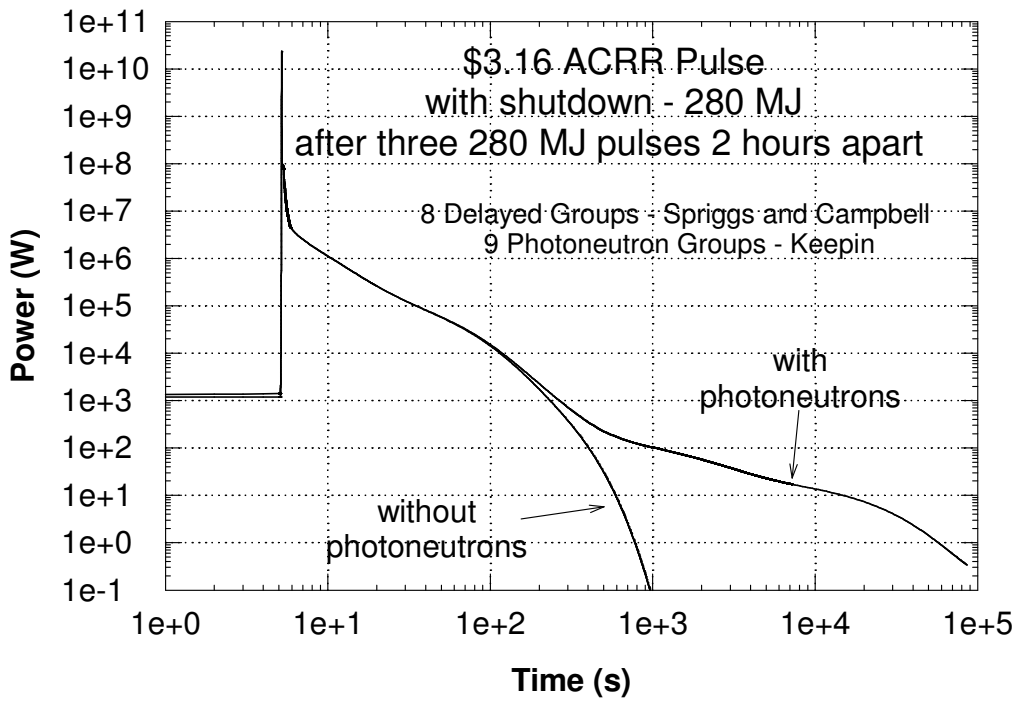


Figure 8. ACRR Power as a Function of Time for a \$3.16 Pulse With and Without Photoneutrons Following a Series of Pulses – Log-Log Scale.

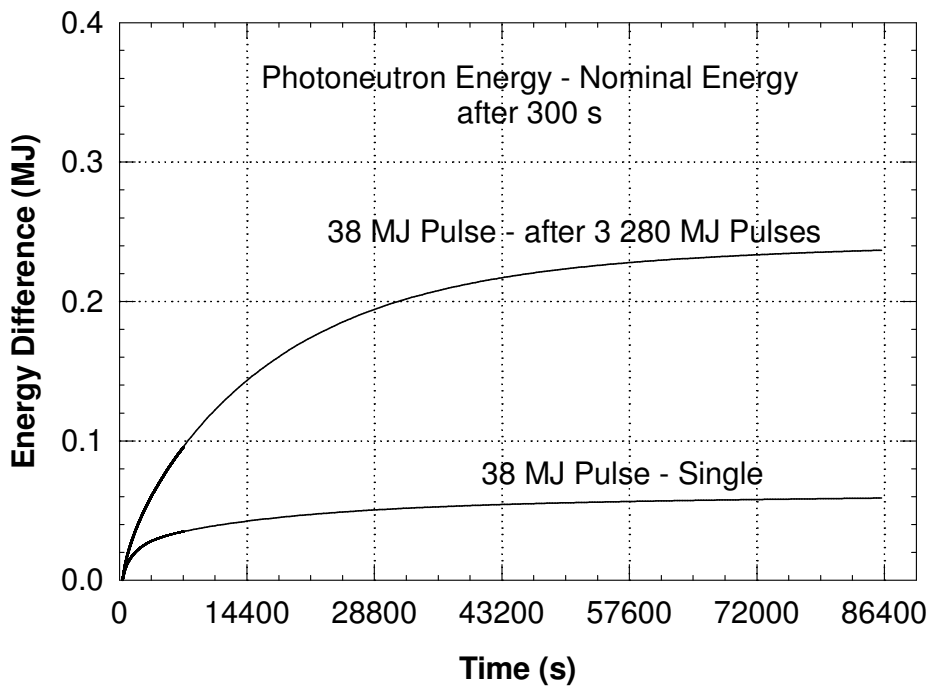


Figure 9. ACRR Power Integrated Over Time as a Function of Time for a \$1.35 Pulse after 300 Seconds – Photoneutron Result Minus Nominal Result.

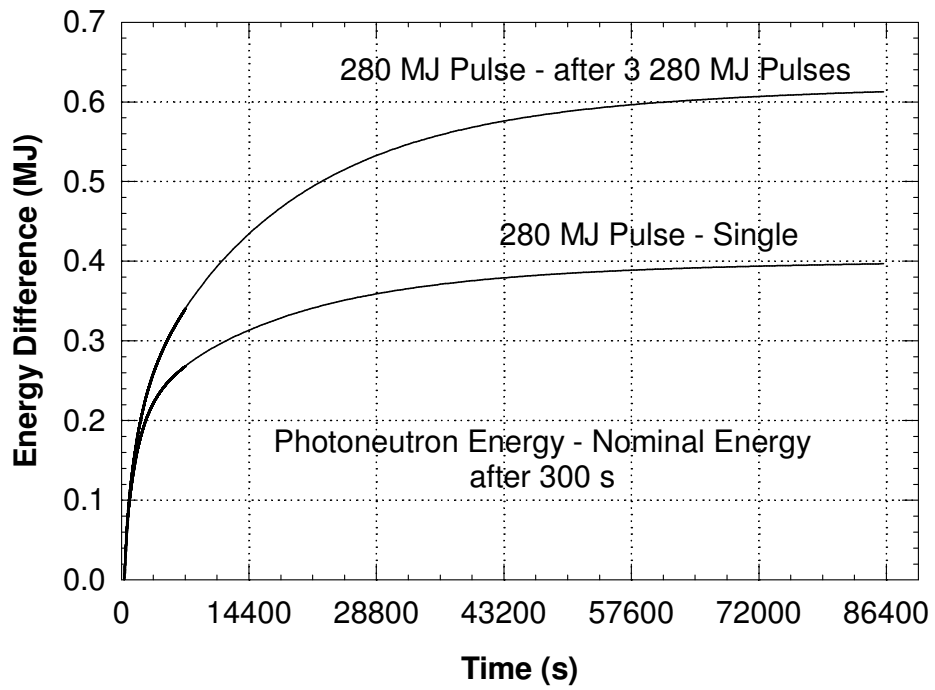


Figure 10. ACRR Power Integrated Over Time as a Function of Time for a \$3.16 Pulse after 300 Seconds – Photoneutron Result Minus Nominal Result.

3.3 Pulse Following a Steady-State Power Run

KIFLHE calculations were also performed to determine the photoneutron effects on the pulse tail following a steady-state power operation at high power for several hours. The condition analyzed was for a 2-MW steady-state power level operation for seven hours followed by a 2-hour decay period and the pulse. For long-power operations, the photoneutron precursors will continue to build up until they reach an equilibrium inventory value. For the fourth group photoneutron precursor, with a half-life of 3.11 hours, about 15 hours of operation would be required in order to reach the equilibrium inventory.

Figures 11 and 12 show the results for a \$1.35 pulse (38 MJ) and a \$3.16 pulse (280 MJ) following a 2-MW – 7-hour steady-state operation with a 2-hour decay period. In order to maintain the correct photoneutron precursor inventory at the start of the pulse calculation, the precursor inventory values, after a 2-hour decay from the end of the steady-state operation, were used as the initial precursor inventory for the calculation. For the \$1.35 pulse case, the power level in the tail is about 300 times greater than for the single pulse value in Figure 6, between 2 and 15 hours following the pulse. For the \$3.16 pulse, the power level is about 50 times larger than for the single pulse value in Figure 2.

Figures 13 and 14 show the integrated power level difference for the \$1.35 pulse case and \$3.16 pulse case, respectively. At 24 hours, the energy deposition is 8.7 MJ and 10.9 MJ, for the two cases. The values are a factor of 140 and 27 times larger than for the single pulse cases, and represent 22% and 4% of the energy deposited in the pulse, for the \$1.35 pulse case and \$3.16 pulse case, respectively. These results are significant compared to the previous cases for a single pulse and a pulse following multiple pulses during the day.

Although the result for a pulse following a high-power steady-state operation for several hours represents the worst case condition for the pulse tail, it is unlikely that this condition would ever be encountered, unless there was a specific experiment requiring this scenario. If a long-power operation is performed, the reactor would probably remain shut down for several days following the run (e.g., over a weekend) allowing the photoneutron precursors to decay to low background levels.

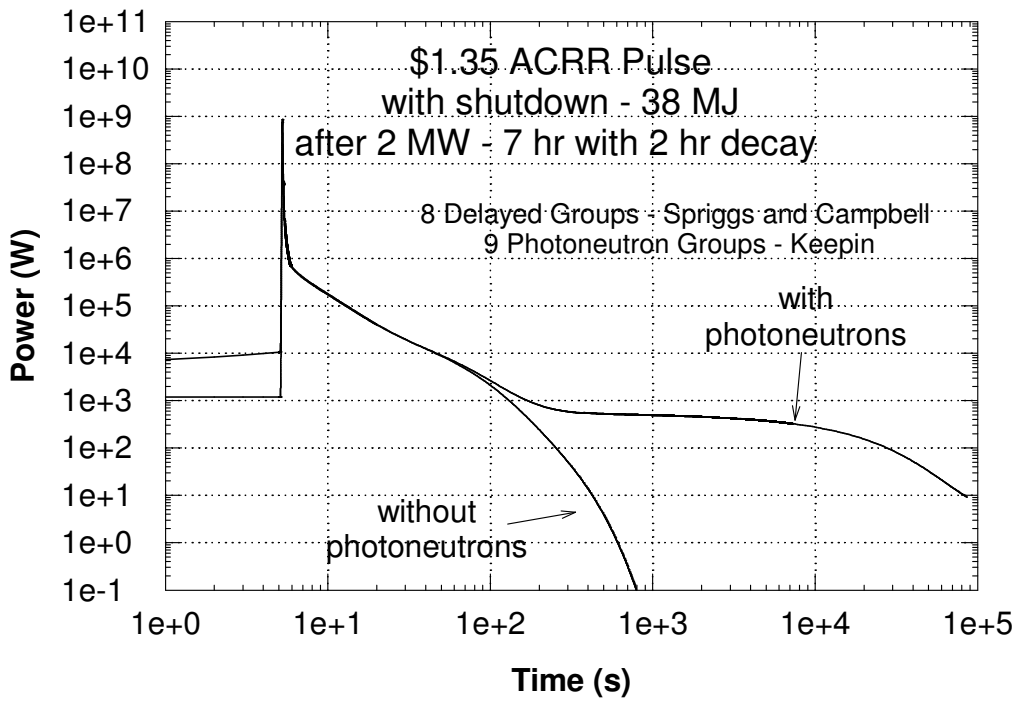


Figure 11. ACRR Power as a Function of Time for a \$1.35 Pulse With and Without Photoneutrons Following 2-MW Steady-State Power Run – Log-Log Scale.

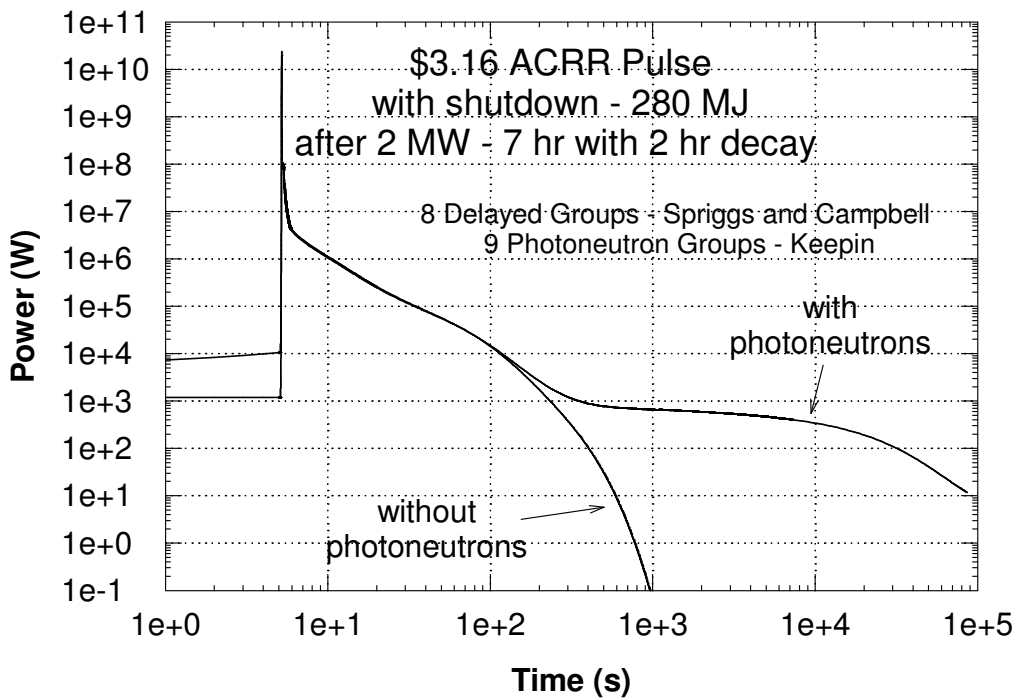


Figure 12. ACRR Power as a Function of Time for a \$3.16 Pulse With and Without Photoneutrons Following 2-MW Steady-State Power Run – Log-Log Scale.

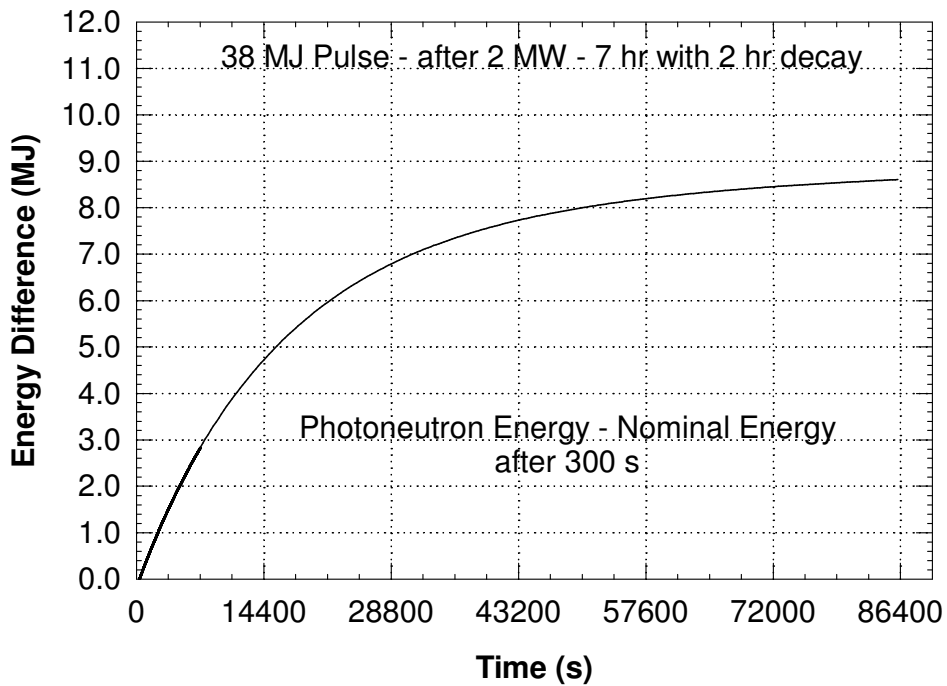


Figure 13. ACRR Power Integrated Over Time as a Function of Time for a \$1.35 Pulse after 300 Seconds – Photoneutron Result Minus Nominal Result.

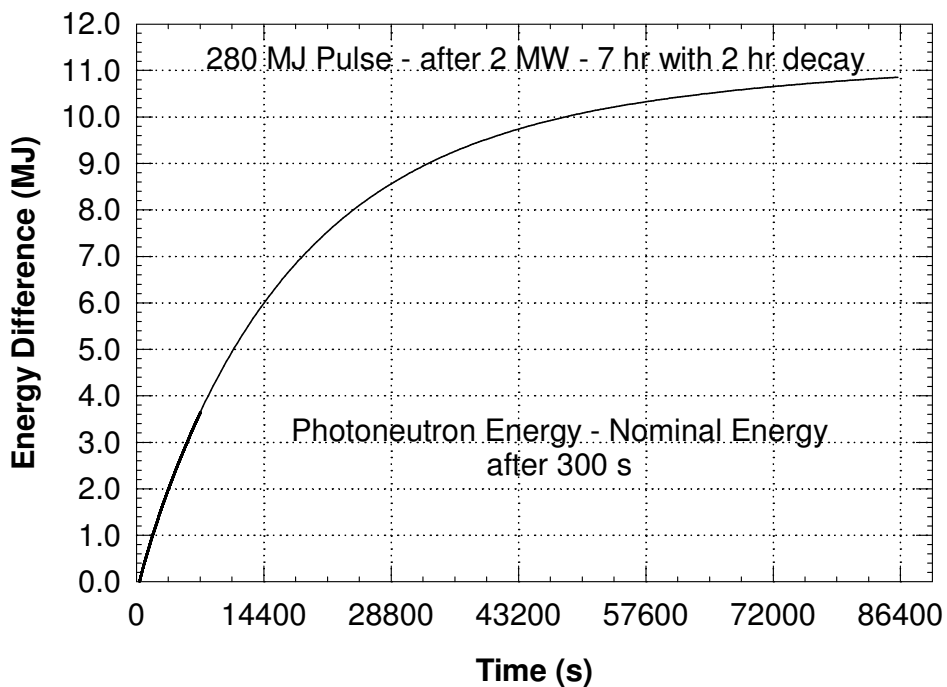


Figure 14. ACRR Power Integrated Over Time as a Function of Time for a \$3.16 Pulse after 300 Seconds – Photoneutron Result Minus Nominal Result.

4 CONCLUSIONS

The KIFLHE transient reactor analysis code has been modified to include the 9-group photoneutron precursor constants of Keepin and the 8-group delayed neutron precursor constants of Campbell and Spriggs. Results indicate that the photoneutron source condition inherent in the ACRR becomes an important contributor to the reactor power level at about 300 seconds following a pulse but contributes less than 1% of the total energy of the pulse. Calculations were performed for a small \$1.35 pulse (38 MJ) and for a large \$3.16 pulse (280 MJ) with and without photoneutrons, and with and without previous pulses or a long-power run. The photoneutron effects persist following a pulse, with the tail decaying with a half-life of about three hours due to one dominant photoneutron precursor. The pulse tail power level and energy are approximately proportional to the energy of the pulse, and continue to increase following each reactor pulse during the day. The pulse tail could be significantly larger for a condition where a pulse follows a high-power steady-state operation for several hours. For this condition, the photoneutron contribution to the pulse energy could be significant, on the order of a few to tens of percent.

Future work could include determining a more accurate representation for the photoneutron group fraction using the MCNP model of the ACRR, since the values used in Table 1 are from experimental data that may be different for the ACRR fuel.

5 REFERENCES

J. M. Campbell, G. D. Spriggs, "8-Group Delayed Neutron Spectral Data for Hansen-Roach Energy Group Structure," LANL99-4000, 1999.

K. R. Depriest, Private Communication, Sandia National Laboratories, September 2008.

G. R. Keepin, Physics of Nuclear Reactor Kinetics, Addison-Wesley Publishing Co., Reading MA, 1965.

J. Lewins, Nuclear Reactor Kinetics and Control, Pergamon Press, New York, NY, 1978.

R. E. Naegeli, E. J. Parma, R. L. Coats, S. W. Longley, and R. X. Lenard, *Safety Analysis Report for the Annular Core Research Reactor Facility*, SAND99-3031, October 1999.

R. E. Naegeli, E. J. Parma, F. M. McCrory, and R. D. Beets, "Addendum to the Safety Analysis Report for the Annular Core Research Reactor Facility (ACRRF), Fuel-Ringed External Cavity, Version II (FREC-II), Experiment Facility for the Annular Core Research Reactor (ACRR)," SAND2000-2147, September 2000.

E. J. Parma, "Analysis for Operating the Annular Core Research Reactor With Cintichem-Type Targets Installed in the Central Region of the Core," SAND99-3200, January 2000.

G. D. Spriggs, J. M. Campbell, V. M. Piksaikin, "An 8-Group Delayed Neutron Model Based on a Consistent Set of Half-Lives," LA-UR-98-1619, Rev. 3, October 1999.

Distribution

1	MS1136	Gary Rochau, 6771
10	MS1136	Ed Parma, 6771
1	MS1141	Jim Dahl, 1383
1	MS1141	Mike Black, 1383
1	MS1141	Dick Coats, 1383
1	MS1141	Mike Gregson, 1383
1	MS1141	Matt Griffin, 1383
1	MS1141	Ron Knief, 1382
1	MS1141	Shivi Singh, 1383
1	MS1142	Darren Talley, 1381
1	MS1142	Matt Burger, 1381
1	MS1142	Lance Lippert, 1381
1	MS1142	Lonnie Martin, 1381
1	MS1142	Tri Trinh, 1381
1	MS1146	Ken Reil, 1384
1	MS1146	Phil Cooper, 1384
1	MS1146	Russell Depriest, 1384
1	MS1146	Pat Griffin, 1384
1	MS1146	Gary Harms, 1384
1	MS1146	Don King, 1384
1	MS1146	Mike Luker, 1384
1	MS1146	Ahti Suo-Anttila, 1384
1	MS0899	Technical Library, 9536 (electronic copy)



Sandia National Laboratories